

Carbon Nanotube Radio

Chris Rutherglen and Peter Burke*

Department of Electrical Engineering and Computer Science, University of California, Irvine, California 92697

Received June 22, 2007; Revised Manuscript Received September 14, 2007

ABSTRACT

Here we report experimental results for a carbon nanotube (CNT) based amplitude-modulated (AM) demodulator for modulation frequencies up to 100 kHz. Further, the CNT based demodulator was successfully demonstrated in an actual AM radio receiver operating at a carrier frequency of 1 GHz and capable of demodulating high-fidelity audio. The demodulation originates from the nonlinear current–voltage (I_{DS} vs V_{DS}) characteristic of the CNT, which induces rectification of a portion of the applied RF signal. By properly biasing the CNT such that the operating point is centered on the maximum nonlinear portion of the I – V curve, one can maximize the demodulation effect. This represents a simple application of carbon nanotubes and nanotechnology to the wireless realm.

The use of carbon nanotubes (CNT) as components in high-frequency electronics has garnered much attention due to their favorable characteristics such as large mobilities, high transconductance, and long mean-free paths. Aside from the popular application of CNTs as high-frequency field-effect transistors,^{1–5} other successful applications include their use as RF detectors and mixers. The use of CNTs as an RF mixer has been demonstrated in various arrangements by Appenzeller et al. and later by Rosenblatt et al. up to 50 GHz, as well as by Pesetki et al. who measured frequency independence up to 23 GHz.^{6–8} All the preceding work utilized the nonlinearity of the drain current with respect to the gate-source $I_D(V_{GS})$ relationship. More recently, Rodriques et al. have demonstrated similar mixer properties of heterodyne microwave detection up to the low gigahertz frequency at $T = 77$ K but this time by taking advantage of the nonlinearity of the source-drain $I_D(V_{DS})$ relationship created by the zero-bias anomaly that manifests at low temperatures.⁹ In this work we utilize room-temperature nonlinearities present in the source-drain $I_D(V_{DS})$ relationship and report experimental results for a carbon nanotube based amplitude-modulated (AM) demodulator with modulation frequencies up to 100 kHz. Our device thus represents a room-temperature two-terminal nonlinear device, simpler than prior three-terminal mixers/detectors. Though not optimized, it represents the first such demonstration, similar to that proposed in Manohara et al.¹⁰ Additionally, we present noise measurements of a CNT RF detector. Finally, the CNT based demodulator was successfully demonstrated in an actual AM radio-receiver demodulating high-fidelity music. This represents a simple application of a CNT that can demonstrate the utility of nanotechnology in the wireless field.

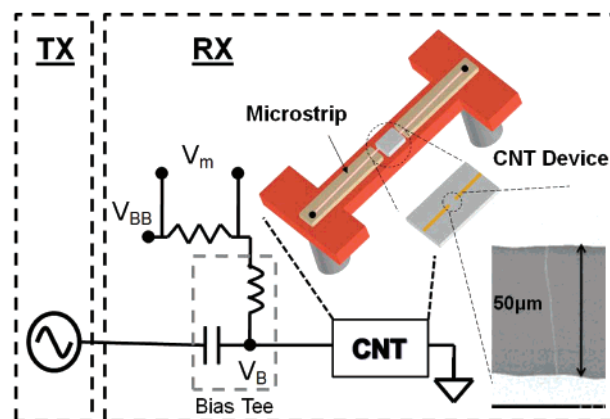


Figure 1. Schematic of the test-setup for the CNT-based AM demodulator. SEM image of a CNT (right).

Carbon nanotubes were synthesized on high resistivity Si wafers ($>8000 \Omega \text{ cm}$) to minimize the detrimental effect of parasitic capacitance at high frequencies. Using optical lithography, catalyst regions were patterned onto the wafer and after 1 h of sonication an aqueous solution of 100 mM FeCl_3 catalyst was applied for 10 s and rinsed with DI water. The CVD growth process is identical to that detailed elsewhere.^{11,12} Subsequent to the nanotube growth, Pd (20 nm)/Au(80 nm) electrodes were evaporated onto the nanotubes with a gap-spacing of $50 \mu\text{m}$ and a width of $300 \mu\text{m}$. Only samples with a single CNT bridging the gap were used for this work. To perform high-frequency measurements the sample device was incorporated on a microwave mount with a pair of SMA connectors and microstrip line connecting the device as shown in Figure 1. A total of four devices with semiconducting CNTs were tested, and all were capable of

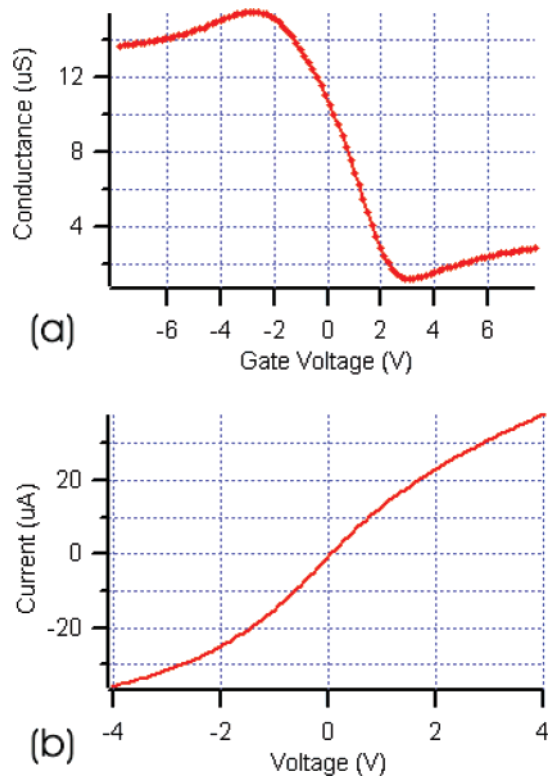


Figure 2. (a) Plot of the source-drain differential conductance vs gate (substrate) voltage of the semiconducting CNT. (b) Current–voltage (I_{DS} vs V_{DS}) curve.

acting as an AM demodulator. The conductance vs gate voltage of the semiconducting CNT under study is presented in Figure 2.

To determine specific features of the nanotube’s use as a demodulator, a simple test setup was devised, as shown in Figure 1. An Agilent E4428C signal generator, with amplitude modulation, functioned as the RF source transmitter (TX) and was fed through a MiniCircuits 0.1–6000 MHz bias tee and into the sample device. Sinusoidal modulation frequencies of 0.01–100 kHz were used to amplitude-modulate (AM) the RF carrier with an 80% modulation depth. The CNT along with a sense resistor and a lock-in amplifier (SR-810) functioned as the receiver (RX) in this setup. Extraction of the modulation signal from the RF carrier was performed by the CNT and the lock-in amplifier, which was tuned to the modulation frequency and used to measure the voltage-drop of the signal across the sense resistor.

The CNT is capable of demodulating an amplitude-modulated RF signal due to its nonlinear current–voltage (I_{DS} vs V_{DS}) characteristics. It can be shown that such nonlinearities can rectify a portion of the applied RF current, which to first order comes out to be

$$I = I_0 \frac{1}{4} \frac{d^2 I}{dV^2} V_{RF}^2 \quad (1)$$

where the voltage of the applied RF signal is V_{RF} , and the second derivative represents the nonlinear current–voltage

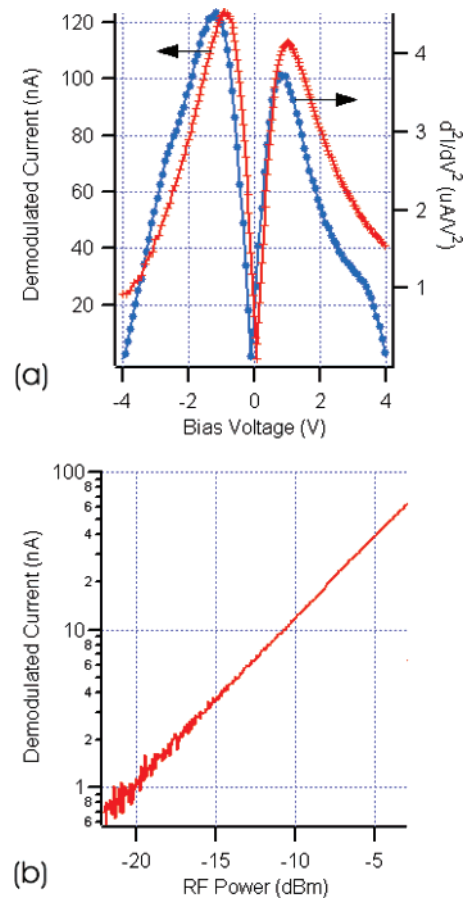


Figure 3. (a) Comparison of demodulated current (red crosses) and $|d^2I/dV^2|$ (blue dots) with respect to the bias voltages, V_B , showing a very good match. (b) Linear modulation current detected by a lock-in amplifier across a 100 k Ω resistor, indicating that I is proportional to V_{RF}^2 ($f = 1$ GHz, $P = 0$ dBm, $f_{mod} = 13$ Hz).

(I_{DS} vs V_{DS}) characteristics of the CNT itself.^{9,13} We found the demodulated signal followed this relationship very well. Comparing the demodulated signal to the absolute value of the numerical second-derivative of the I – V trace shown in Figure 2b, we see in Figure 3a that the two are nearly identical in form supporting that $I_{rectified} \propto d^2I/dV^2$. Further, the proportionality relationship between detected output signal and the applied RF power (which itself is proportional to V_{RF}^2) was measured to be linear, indicating that $I_{rectified} \propto V_{RF}^2$, as shown in Figure 3b.

Maximizing the demodulated signal can be achieved through proper biasing of the CNT. As evident in Figure 3a, one can obtain maximum demodulation by biasing the CNT such that the operating point is centered on the maximum nonlinear portion of the I – V curve. Due to the inherent symmetry of the nanotube, two such operating points exist at ± 1 V. The maximum current responsivity was measured to be 125 nA/mW and was found to be independent of back-gate voltage.

Considering that the CNT resistance is on the order of 100 k Ω , from an RF point of view, a large impedance mismatch will exist between the CNT and the 50 Ω characteristic impedance of the transmission line, resulting in a strong microwave signal reflection off the CNT. Because

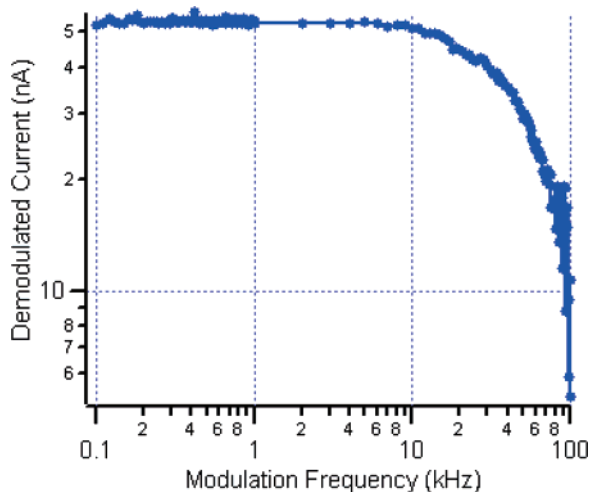


Figure 4. Demodulated current amplitude as measured with respect to the modulation frequency ($f = 1$ GHz, $P_{wr} = -5$ dBm, $R = 100 \Omega$, and $V_{BB} = 2$ V).

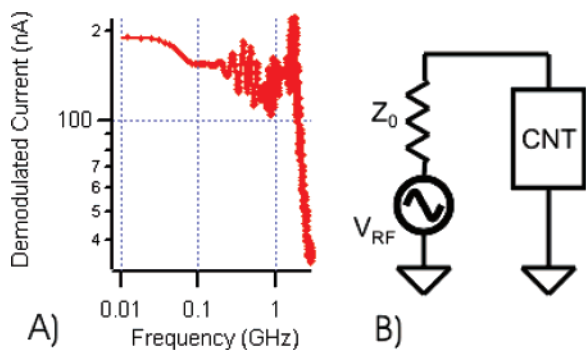


Figure 5. (A) Demodulated signal at various frequencies. Parasitic capacitance shorts the RF signal at frequencies > 2 GHz. (B) Schematic of RF equivalent circuit.

the power available from the source is $P_{AVS} = V_{RF}^2/8Z_0$, and the RF voltage at the CNT is V_{RF} due to $Z_{CNT} \gg Z_0$, using eq 1, we obtain $I/P_{AVS} = 2(d^2I/dV^2)Z_0$ for the responsivity of the CNT demodulator. The circuit for this analysis is presented in Figure 5B. This indicates that the resistance of the CNT is independent of the device's responsivity insofar as the second derivative of the CNT is the same. Taking the maximum measured value for second-derivative as $4 \mu A/V^2$, one arrives at a responsivity of 400 nA/mW , which is comparable to the measured value of 125 nA/mW .

The effectiveness of the device at detecting the modulation signal up to 100 kHz was found to be limited by extrinsic parameters of the experimental setup and not due to the CNT itself. Due to capacitance within the bias tee and coax cable in conjunction with the sense resistor, an RC low-pass filter was established, thus giving a roll-off in the high audio frequency range of the demodulated signal. To minimize this effect, the detection resistor and the bias-tee's capacitor were reduced to 100Ω and 100 pF , respectively. The roll-off was measured to have a -3 dB corner at 40 kHz , as shown in Figure 4, which is well above the upper range of human hearing. Signal loss due to the inductor of the bias tee was measured to be -1.5 dB at 100 kHz , which is rather insignificant compared to the other sources of attenuation.

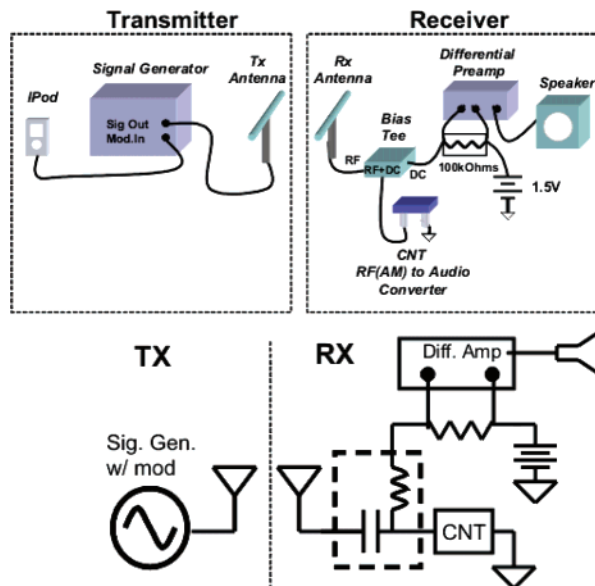


Figure 6. Schematic of CNT radio demonstration.

As expected, at high carrier frequencies (> 2 GHz) the parasitic capacitance resulted in a strong degradation in the received signal (Figure 5A). This is predominantly due to the relatively large contact pads used ($300 \mu\text{m} \times 1000 \mu\text{m}$).

Noise measurements were performed on the CNT demodulator system operating at a carrier frequency of 1 GHz and bias voltage of 2.5 V . The system voltage-noise density, which includes noise from the lock-in amplifier, sense-resistor, and CNT was measured to be $40 \times 10^{-9} \text{ (V/Hz}^{1/2})$ at an audio frequency of 1 kHz . Using the measured responsivity, β_I , of 125 nA/mW together with the device resistance of $100 \text{ k}\Omega$, the noise-equivalent power (NEP) is calculated using $\text{NEP} = v_n/(\beta_I R) \text{ (W/Hz}^{1/2})$ and is $3 \text{ nW/Hz}^{1/2}$. This puts an upper limit on the noise equivalent power of the CNT itself.

Utilizing the above documented effect, we demonstrate a simple design for a CNT based radio receiver (see Figure 6). Here the carbon nanotube functions in the critical role as the receiver's AM demodulator. The transmitter portion of the demo utilizes a signal generator to create a 1 GHz RF signal that is externally amplitude modulated (AM) with music by an iPod and fed to a dipole antenna for wireless broadcast (see Supporting Information). On the receiver side, the RX antenna picks up the 1 GHz RF signal, feeding it through a bias-tee and onto the carbon nanotubes where it is rectified. The distance between the TX and RX antennas was limited to $\sim 1 \text{ m}$, but that can be improved by simply including a standard front-end preamplifier to boost the received signal before sending it on to the CNT for demodulation. A 1.5 V battery is used to properly bias the CNT for maximum demodulation. A differential pre-amplifier then amplifies the voltage drop across a sense resistor, and the high-fidelity audio is fed to a speaker for audio broadcast. The audio-quality of the signal demodulated by the CNT was very clear and indistinguishable to the human ear from listening to the music directly (see Supporting Information).

To predict how to optimize device performance as a function of length, one would need a quantitative and detailed

theory of nanotube I – V curves, and their nonlinearity. Although numerical simulation code exists that can predict nanotube I – V curves, a detailed study of the nonlinearity of CNTs as a function of length has not yet been performed. In the absence of such studies, we may predict on the basis of general physical principles methods to optimize the CNT length to maximize the nonlinearity.

Considering that the nonlinearity in I – V originates from phonon scattering processes, one can further optimize the responsivity of the CNT demodulator by maximizing this nonlinear influence.^{14–16} In general, this can be accomplished by decreasing the length of the nanotube to an optimum value. Depending whether one is in the low or high voltage bias regime, the dominant scattering mechanism would be acoustic phonon scattering or optical phonon scattering, respectively. In the limit of each of these regions the slope of the nanotube's I_{DS} vs V_{DS} curve can be expressed as $G = (4e^2/h) \times l_i/(l_i + L)$, where L is the nanotube length and l_i equals $l_{ap} \sim 300$ nm for acoustic phonon scattering in the low bias regime and $l_{op} \sim 15$ nm for optical phonon scattering in the high bias regime.¹⁶ The nonlinearity manifests as the bias voltage transitions from a region with one dominated scattering mechanism to the other, which in general can be maximized by considering what length nanotube, L , would result in the greatest difference in the slope of I – V between the two regions. For example, if we consider the mean-free-path lengths stated above to be generally accurate, the difference in the slopes is maximized when the nanotube length is ~ 100 nm. If the nanotube length is decreased further, ballistic transport dominates and the nonlinearity in I – V is again reduced. For long nanotubes ($> 10 \mu\text{m}$) other scattering processes would become significant such as defect induced elastic scattering, which further complicates the analysis. Other mechanisms typically responsible for nonlinear I – V characteristics such as a Schottky barrier at the contacts were of negligible contribution due to the use of Pd ohmic contacts.¹⁷ Furthermore, because both metallic and semiconducting CNTs display this behavior, these scaling arguments could be applied to both cases. Thus, although the observed nonlinearity is rather mild, it can be dramatically improved through careful optimization.

We have successfully demonstrated and analyzed the use of a carbon nanotube to demodulate an AM (amplitude modulation) microwave signal in the application of an AM radio receiver. As such, this work represents a step toward a *systems* demonstration as opposed to a device demonstration, an important step that addresses the field of *nanotechnology*, as opposed to *nanoscience*. Though we have only demonstrated the *critical* component of the entire radio system out of a nanotube (the demodulator), it is conceivable in the future that *all* components could be nanoscale, thus allowing a truly nanoscale wireless communications system, as we envisioned in ref 18. Thus, this work takes a step toward enabling such an *integrated nanosystem*.

Acknowledgment. This work was supported by the Army Research Office and the Office of Naval Research.

Note Added after ASAP Publication. Since Web publication of this manuscript the authors have become aware of

similar work demonstrating nanotube radio performance at UIUC in the group of Professor John Rogers.¹⁹ Manuscript was originally published ASAP October 17, 2007; the updated version was published October 30, 2007.

Supporting Information Available: An avi video demonstration of the CNT radio. This material is available free of charge via the Internet at <http://pubs.acs.org>.

References

- (1) McEuen, P. L.; Fuhrer, M. S.; Park, H. K. Single-walled carbon nanotube electronics. *IEEE Transactions on Nanotechnology* **2002**, *1* (1), 78–85.
- (2) Burke, P. J. AC performance of nanoelectronics: towards a ballistic THz nanotube transistor. *Solid State Electronics* **2004**, *40* (10), 1981–1986.
- (3) Le Louarn, A. F. K.; Bethoux, J.-M.; Happy, H.; Dambrine, G.; Derycke, V.; Chenevier, P.; Izard, N.; Goffman, M. F.; Bourgoin, J.-P. Intrinsic current gain cutoff frequency of 30 GHz with carbon nanotube transistors. *Appl. Phys. Lett.* **2007**, *90*, 233108.
- (4) Kang, S. J.; Kocabas, C.; Ozel, T.; Shim, M.; Pimparkar, N.; Alam, M. A.; Rotkin, S. V.; Rogers, J. A. High-performance electronics using dense, perfectly aligned arrays of single-walled carbon nanotubes. *Nature Nanotechnology* **2007**, *2* (4), 230–236.
- (5) Wang, D.; Yu, Z.; McKernan, S.; Burke, P. Ultra High Frequency Carbon Nanotube Transistor Based on a Single Nanotube. *IEEE Trans. Nanotechnol.* **2007**, *6* (4), 400–403.
- (6) Pesetski, A. A.; Baumgardner, J. E.; Folk, E.; Przybysz, J. X.; Adam, J. D.; Zhang, H. Carbon nanotube field-effect transistor operation at microwave frequencies. *Appl. Phys. Lett.* **2006**, *88* (11), 113103.
- (7) Appenzeller, J.; Frank, D. J. Frequency dependent characterization of transport properties in carbon nanotube transistors. *Appl. Phys. Lett.* **2004**, *84* (10), 1771–1773.
- (8) Rosenblatt, S.; Lin, H.; Sazonova, V.; Tiwari, S.; McEuen, P. Mixing at 50 GHz using a single-walled carbon nanotube transistor. *Appl. Phys. Lett.* **2005**, *87*, 15311.
- (9) Rodriguez-Morales, F.; Zannoni, R.; Nicholson, J.; Fischetti, M.; Yngvesson, K. S.; Appenzeller, J. Direct and heterodyne detection of microwaves in a metallic single wall carbon nanotube. *Appl. Phys. Lett.* **2006**, *89* (8), 083502-1–083502-3.
- (10) Manohara, H. M.; Wong, E. W.; Schlecht, E.; Hunt, B. D.; Siegel, P. H. Carbon nanotube Schottky diodes using Ti-Schottky and Pt-Ohmic contacts for high frequency applications. *Nano Lett.* **2005**, *5* (7), 1469–1474.
- (11) Yu, Z.; Li, S.; Burke, P. J. Synthesis of aligned arrays of millimeter long, straight single walled carbon nanotubes. *Chem. Mater.* **2004**, *16* (18), 3414–3416.
- (12) Li, S.; Yu, Z.; Rutherglen, C.; Burke, P. J. Electrical properties of 0.4 cm long single walled carbon nanotubes. *Nano Lett.* **2004**, *4* (10), 2003–2007.
- (13) Pozar, D. M. *Microwave Engineering*; Wiley: New York, 1998.
- (14) Yao, Z.; Kane, C. L.; Dekker, C. High-field electrical transport in single-wall carbon nanotubes. *Phys. Rev. Lett.* **2000**, *84* (13), 2941–2944.
- (15) Park, J. Y.; Rosenblatt, S.; Yaish, Y.; Sazonova, V.; Ustunel, H.; Braig, S.; Arias, T. A.; Brouwer, P. W.; McEuen, P. L. Electron-phonon scattering in metallic single-walled carbon nanotubes. *Nano Lett.* **2004**, *4* (3), 517–520.
- (16) Javey, A.; Guo, J.; Paulsson, M.; Wang, Q.; Mann, D.; Lundstrom, M.; Dai, H. J. High-field quasiballistic transport in short carbon nanotubes. *Phys. Rev. Lett.* **2004**, *92* (10), 106804-1–106804-4.
- (17) Javey, A.; Guo, J.; Wang, Q.; Lundstrom, M.; Dai, H. J. Ballistic carbon nanotube field-effect transistors. *Nature* **2003**, *424* (6949), 654–657.
- (18) Burke, P. J.; Li, S. D.; Yu, Z. Quantitative theory of nanowire and nanotube antenna performance. *IEEE Trans. Nanotechnol.* **2006**, *5* (4), 314–334.
- (19) Rogers, J.; et al. Unpublished work.

NL0714839